Optica Applicata, Vol. XXXV, No. 2, 2005

Transparent $(1-x)TiO_2-xFe_2O_3$ (x = 0, 5, 10, 15 and 20 mol%) thin films prepared by sol-gel process

KYU-SEOG HWANG[1], YOUNG-SUN JEON[1, 2], KYUNG-OK JEON[1,2], BYUNG-HOON KIM[2]

[1]Department of Applied Optics and Institute of Photoelectronic Technology, Nambu University, 864-1 Wolgye-dong, Gwangsan-gu, Gwangju 506-824, Republic of Korea

[2]Department of Materials Science & Engineering, Chonnam National University, 300 Yongbong-dong, Buk-gu, Gwangju 500-757, Republic of Korea; e-mail: bhkim@cnu.ac.kr

Transparent iron-doped titanium oxide thin films were prepared on soda-lime-silica glass substrate from a titanium naphthenate precursor. Films prefired at 500°C for 10 min were finally annealed at 500°C for 30 min in air. Field emission–scanning electron microscope and scanning probe microscope were used for characterizing the surface structure of the film. A sharp absorption edge of the film was observed. The film containing iron showed a shift towards the visible in the absorption threshold.

Keywords: titanium oxide, thin film, iron.

1. Introduction

Titanium oxide TiO_2 has universally been recognized as one of the better photocatalysts in heterogeneous photocatalysis applications as it combines two important complementary features for a photocatalyst: good UV absorption efficiency for the light harvesting process and good adsorption capacities, due particularly to the density of OH^- groups of amphoteric character. However, the band gap energy requires that near-UV light be used to photo activate this very attractive photocatalyst [1–3]. Unfortunately, in solar energy applications only ~3% of the solar light is absorbed. It would be advantageous, therefore, if this metal oxide semiconductor (SC) could be photosensitized by visible light.

Doping TiO_2 with Fe or other metal cations has been attempted for photocatalytic applications by shifting the threshold for photonic excitation of the titanium oxide towards the visible. These systems are being prepared in the form of thin films due to the advantages of their use as electrodes, transparent coatings, *etc*. [4–6]. However, as far as we know, there is little information to prepare Fe-doped TiO_2 thin films by chemical solution deposition (CSD).

In this study, we report on the preparation of transparent Fe-doped TiO_2 thin films on soda-lime-silica glass (SLSG) substrate by CSD using metal naphthenate precursor.

2. Experimental procedure

The preparation for the TiO_2 thin films from titanium naphthenate is described in detail in our previous work [7]. Briefly, a precursor sol was prepared using Ti- and Fe-naphthenates (Nihon Kagaku Sangyo Co., Ltd., Japan) and by diluting the sol with toluene (concentration: 4 wt% metal/100 ml sol). The iron contents, as mol percentage, were 0, 5, 10, 15, and 20. Samples are denoted as T100, T95F5, T90F10, T85F15, and T80F20, the numbers after the letters give the nominal total titanium and iron contents expressed as mol percentage. SLSG was cleaned in distilled water, immersed in H_2O_2 and finally rinsed in toluene. The precursor sol was spin coated onto the cleaned SLSG at 1500 rpm for 10 sec. The as-deposited film was prefired at 500°C for 10 min in air. The coating process was repeated five times. A final annealing was performed at 500°C for 30 min in air by directly inserting the samples into a preheated tube-type furnace, followed by fast cooling.

The crystallinity of the annealed film was examined by high resolution X-ray diffraction system (HRXRD, X'pert-PRO, Philips, Netherlands). Transmittance in the visible wavelength range was observed by using a UV-visible-NIR spectrophotometer (Cary 500 Scan, Varian Co., Australia). The thickness of the annealed film was determined by observation of fracture-cross sections by means of a field emission–scanning electron microscope (FE-SEM, S-4700, Hitachi Co., Japan) and F20 (Filmetric Inc., San Diego, U.S.A.) using reflection spectrum. The surface structure of the film was studied with FE-SEM and a scanning probe microscope (SPM, XE-200, PSIA, Korea). All the SPM measurements were performed in air using the tapping mode. The hydrophilic property of the films was evaluated by examining the contact angle between water and the films. Irradiation in the UV wavelength range was performed using an UV lamp (UVGL-58, UVP Co., U.S.A.) at 1.0 mW/cm^2. Contact angles were measured with horizontal microscope with a protractor eyepiece at room temperature (contact angle micrometer, CAM Plus-Micro×12, Tantec Inc., U.S.A.). Water droplets were placed at five different positions for one sample and the averaged value was adopted as the contact angle.

3. Results and discussion

Figure 1 shows the XRD curve of the films deposited on SLSG substrate. The XRD pattern of T100 and T95F5 consists of only anatase peaks such as (110) reflections. The films after prefiring exhibit amorphous character, not shown here. By contrast, peak intensity of the anatase TiO_2 comparatively decreased for the sample containing iron (T90F10, T85F15 and T80F20). From XRD result, we can assume that iron forms a solid solution in the TiO_2 structure and that there is no iron oxide precipitated as secondary phase when making a solid solution with TiO_2.

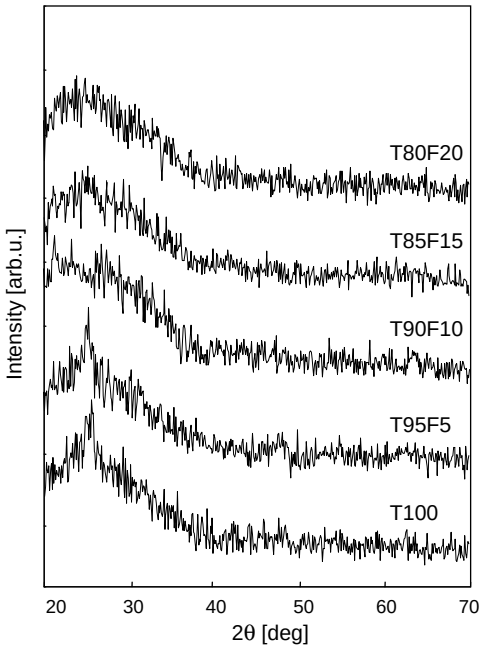

Fig. 1. XRD patterns of the films on SLSG substrates after annealing at 500°C.

There is an interesting difference in the crystalline structure between pure TiO_2 and Fe-doped TiO_2 samples. Pure TiO_2 thin film was crystallized into the anatase structure. By contrast, the films containing Fe yielded amorphous structure for the film with the Fe content above 10 mol%.

Many transition metals, such as Fe, Ni, V, Cr and Co are known to promote the anatase-rutile transition in TiO_2 [8]. This enhancement effect has been explained on the basis of M^+ (M = metal) diffusion into the TiO_2 lattice, which generates the oxygen vacancies that are needed to maintain charge neutrality, favoring rutile nucleation. These oxygen vacancies are responsible for the enhancement of transformation from anatase to rutile [8]. However, in this work, it is very difficult to identify crystalline phases in the films containing high Fe-doping mol%. We assume that lower annealing temperature, 500°C, was insufficient for transformation from anatase to rutile.

Figure 2 shows FE-SEM photographs for the films on SLSG substrates finally annealed at 500°C. Particulate structure is evident in Fe-doped TiO_2 film. The particle size increases with an increase of iron doping mol%. It is noted that no evidently aggregated particles are present and the nano-sized particles were obtained in all the films except 20 mol% Fe-doped TiO_2 film annealed at 500°C. Generally, in the CSD method, pores and cracks are easily recognized in the product films. On the contrary, the surface of the film produced in this work was flat and smooth.

Figure 3 shows FE-SEM images for the fractured cross-section of the T95F5 and T80F20 thin films. The interfaces between the films and the substrates were very flat and homogeneous. The thickness tended to increase with increasing the Fe-doping mol%, being 523, 541, 580, 634 and 691 nm for the films T100, T95F5, T90F10,

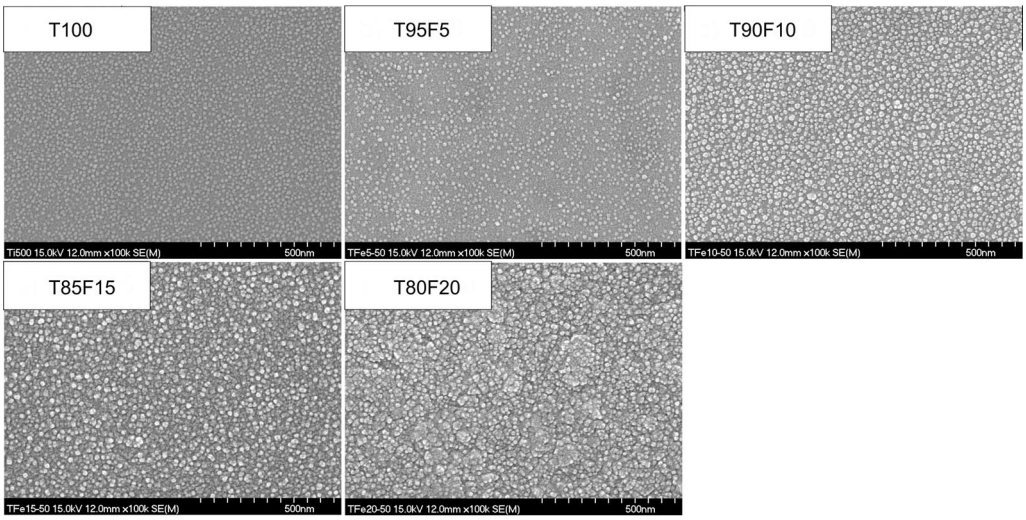

Fig. 2. FE-SEM photographs of the films on SLSG substrates after annealing at 500°C.

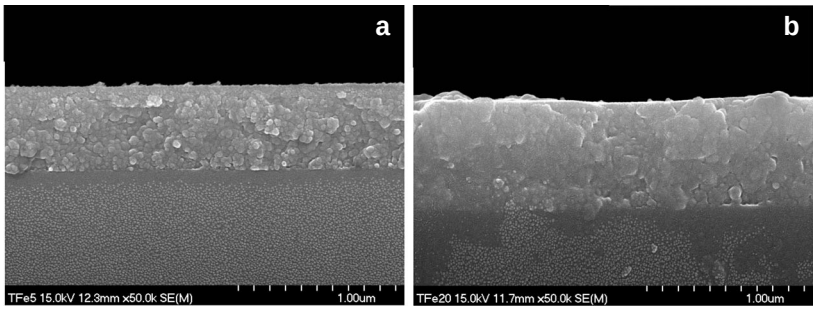

Fig. 3. FE-SEM photographs for the fractured cross-section of the films T95F5 (**a**) and T80F20 (**b**) after annealing at 500°C.

T85F15, and T80F20, respectively. Thickness of the film was increased with Fe-doping mol%. We assume that an increase of the viscosity of the coating sol induced variation of the film thickness according to the Fe-doping mol% since Fe-naphthenate was stickier than Ti-naphthenate in appearance.

To evaluate the surface topology of the films according to Fe-doping mol%, SPM analysis was performed. Figure 4 shows the SPM images of the films on SLSG substrate annealed at 500°C. The surface of T100 is composed of relatively low-surface roughness without 3-dimensional grain outgrowth, as shown in Fig. 4. Furthermore, for the Fe-doped TiO_2 thin films, it is difficult to identify large grain outgrowth, such as island growth on the 2-dimensionally grown layer. The smoothness of the surface of the films from SPM analysis is relatively high. On the other hand, in our previous work, the TiO_2 film coated on SLSG substrate exhibited needle-shape grain outgrowth

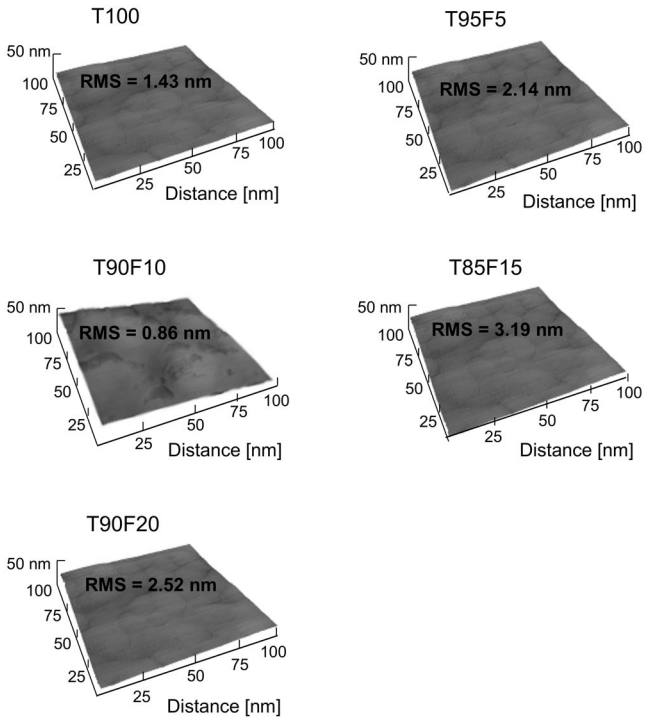

Fig. 4. SPM images of the films on SLSG substrates after annealing at 500°C.

owing to nonstoichiometry of the TiO_2 film annealed at 600°C [7]. We assumed that formation of the second phases was caused by sodium or calcium diffusion near the interface between TiO_2 and SLSG substrate [7]. We can conclude that low-temperature annealing at 500°C was sufficiently effective to suppress alkali-diffusion from the substrate used.

Figure 5 shows the visible spectra in the wavelength range 300–900 nm of the films on SLSG substrates annealed at 500°C. Relative high transmittance at visible range and a clear absorption edge of the film were observed. The high transmittance of the film is attributed to the small particle size which eliminates light scattering [7]. From these spectra, it is apparent that films present relatively high optical quality, with an absorption in the visible region that is characterized by the typical interference pattern found when a transparent thin film is deposited onto a substrate of different refractive index. Furthermore, the film containing iron showed a clear shift towards the visible in the absorption threshold. This shift was higher as the amount of iron in the films increased.

The optical absorption coefficient α, is defined as,

$$I = I_0 \exp(-\alpha t) \tag{1}$$

where I is the intensity of transmitted light, I_0 is the intensity of incident light, and t is the thickness of TiO_2 film. Since the transmittance is defined as I/I_0, we obtain α

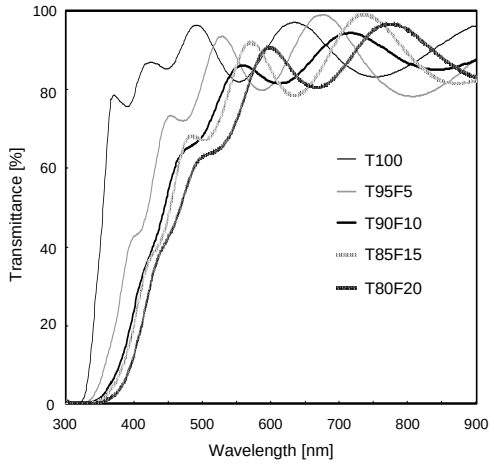

Fig. 5. Transmittance of the films on SLSG annealed at 500°C.

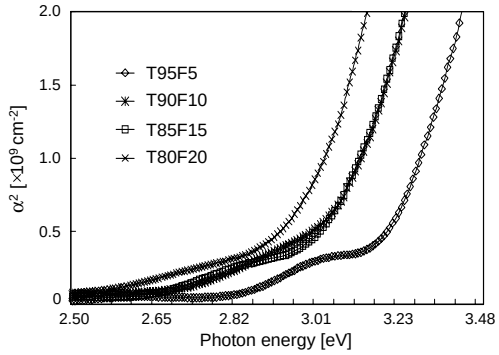

Fig. 6. Square of the absorption coefficient as a function of photon energy for the films on SLSG substrates after annealing at 500°C.

from Eq. (1). In the direct transition semiconductor, α and optical energy band gap E_g are related by [9]

$$\alpha = (h\nu - E_g)^{1/2} \tag{2}$$

where h is Planck constant, and ν is the frequency of the incident photon. As shown in Fig. 6, the linear dependence of α^2 on $h\nu$ indicates that films on SLSG are the direct transition-type semiconductor. The photon energy at the point where α^2 is zero is E_g. Then E_g is determined by the extrapolation method [10]. Optical band gap E_g is in the range between 3.696 eV and 3.018 eV, as shown in Fig. 7. The estimated value of the band gap for the T100 is larger than that of TiO_2 bulk (3.3 eV). The film consisting of fine crystallites shows *blue shift* [11]. We assume that the increase in the band gap is due to the quantum size effect (QSE), which occurs for semiconductor particles below 100 nm. Moreover, it can be clearly observed that for each sample the band gap energy decreases with an increase of Fe-doping mol%, as shown in Fig. 7.

A comparison of optical energy gaps between pure TiO_2 and Fe-doped TiO_2 thin films shows an obvious red shift in Fe-doped TiO_2 films at the same annealing

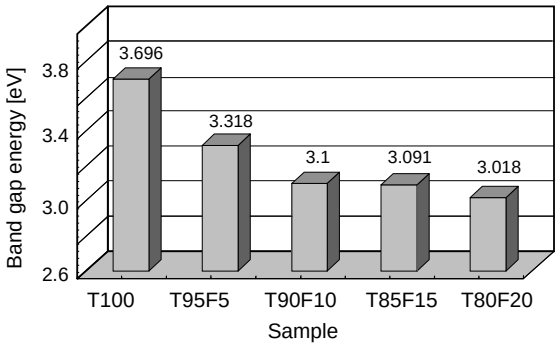

Fig. 7. Band gap energy for the films on SLSG substrates after annealing at 500°C.

temperature. The large red shift in optical energy gaps is considered due to two factors. The first comes from the mixture effect of band gap of composite semiconductor. When TiO_2 with a relatively high band gap is mixed with a low band gap Fe_2O_3, the band gap of the composite semiconductor Fe-doped TiO_2 will locate between these two materials, *i.e.*, the shift to lower energy compared with pure TiO_2 thin film. The second one is considered due to the interface effect between Fe_2O_3 and TiO_2 particles, TiO_2 particles are isolated by Fe_2O_3 particles and the increased dielectric confinement effect at the interface can also cause the red shift [4].

The contact angle was being measured to examine the surface wettability of the thin films. Figure 8 shows the time dependence of the water contact angle of the films upon UV illumination. When UV light shone on the film surface for above 45 min, the surface gradually converted to a hydrophilic state. Stored in the dark for 300 min, the surface gradually reconverts to the hydrophobic state. The hydrophobic to hydrophilic state conversion is explained by assuming that surface Ti^{4+} sites are photoinduced to the Ti^{3+} state [12]. This process is essentially the same as the surface

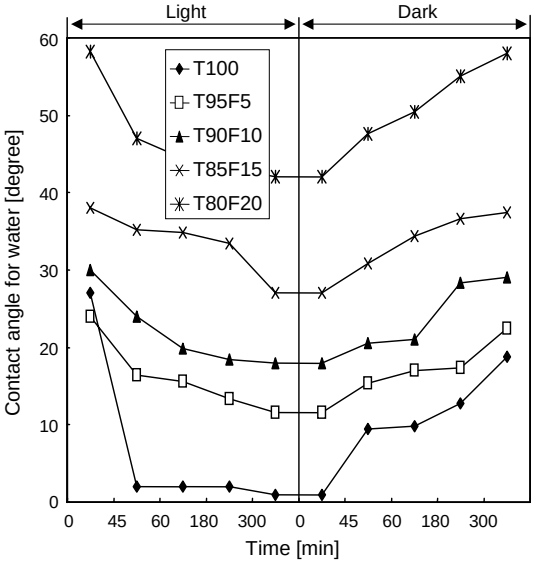

Fig. 8. Hydrophilic–hydrophobic conversion upon UV illumination and storage in dark films on SLSG substrates after annealing at 500°C.

reduction process of Ti^{4+} to Ti^{3+} induced by Ar ion sputtering [13] and electron beam exposure [14]. However, the films containing iron showed high contact angle despite sufficient UV illumination time, 300 min. The best hydrophilicity was achieved with a pure TiO_2 film. The hydrophilicity of the high doping TF films was not preferable.

4. Conclusions

Pure TiO_2 and Fe-doped TiO_2 thin films were prepared on SLSG substrate at 500°C from metal naphthenate precursor. The surface of the films showing a high transmittance at the visible wavelength range is composed of relatively high surface smoothness without grain outgrowth. A comparison of optical energy gaps between pure TiO_2 and Fe-doped TiO_2 thin films shows an obvious red shift in Fe-doped TiO_2 films at the same annealing temperature. With an increase of Fe content on the film, the contact angle for water increased.

References

[1] ZAHARESCU M., CRISAN M., MUŠEVIČ I., *Atomic force microscopy study of TiO_2 films obtained by the sol-gel method*, Journal of Sol-Gel Science and Technology **13**(1-3), 1998, pp. 769–73.

[2] NISHIDE T., SATO M., HARA H., *Crystal structure and optical property of TiO_2 gels and films prepared from Ti-edta complexes as titania precursors*, Journal of Materials Science **35**(2), 2000, pp. 465–9.

[3] KIM B.H., AN J.H., KANG B.A., HWANG K.S., OH J.S., *Preparation of TiO_2 layer by spin coating-pyrolysis and in-vitro formation of calcium phosphate*, Journal of Ceramic Processing Research **5**(1), 2004, pp. 53–7.

[4] LI G.H., YANG L., JIN Y.X., ZHZNG J.D., *Structural and optical properties of TiO_2 thin film and TiO_2+2 wt.% $ZnFe_2O_4$ composite film prepared by r.f. sputtering*, Thin Solid Films **368**(1), 2000, pp. 163–7.

[5] GRACIA F., HOLGADO J.P., YUBERO F., GONZÁLEZ-ELIPE A.R., *Phase mixing in Fe/TiO_2 thin films prepared by ion beam-induced chemical vapour deposition: Optical and structural properties*, Surface and Coatings Technology **158-159**, 2002, pp. 552–7.

[6] CHOI W., TERMIN A., HOFFMANN M.R., *Role of metal ion dopants in quantum-sized TiO_2. Correlation between photoreactivity and charge carrier recombination dynamics*, Journal of Physical Chemistry **98**(51), 1994, pp. 13669–79.

[7] RYU H.W., PARK J.S., HONG K.J., HWANG K.S., KANG B.A., OH J.S., *Nanocrystalline TiO_2 thin films on soda-lime-silica glass by using a titanium naphthenate precursor*, Surface and Coatings Technology **173**(1), 2003, pp. 19–23.

[8] RIYAS S., YASIR V.A., DAS P.N.M., *Crystal structure transformation of TiO_2 in presence of Fe_2O_3 and NiO in air atmosphere*, Bulletin of Materials Science **25**(4), 2002, pp. 267–73.

[9] PARK K., MA D., KIM K., *Physical properties of Al-doped zinc oxide films prepared by RF magnetron sputtering*, Thin Solid Films **305**(1-2), 1997, pp. 201–9.

[10] SHIMONO D., TANAKA S., TORIKAI T., WATARI T., MURANO M., *Preparation of transparent and conductive ZnO films using a chemical solution deposition process*, Journal of Ceramic Processing Research **2**(4), 2001, pp. 184–8.

[11] WANG T., WANG H., XU P., ZHAO X., LIU Y., CHAO S., *Effect of properties of semiconductor oxide thin films on photocatalytic decomposition of dyeing waste water*, Thin Solid Films **334**(1-2), 1998, pp. 103–8.

[12] WANG R., HASHIMOTO K., FUJISHIMA A., CHIKUNI M., KOJIMA E., KITAMURA A., SHIMOHIGOSHI M., WATANABE T., *Photogeneration of highly amphiphilic TiO_2 surfaces*, Advanced Materials **10**(2) 1998, pp. 135–8.

[13] HUGENSCHMIDT M.B., GAMBLE L., CAMPBELL C.T., *Interaction of H_2O with a TiO_2(110) surface*, Surface Science **302**(3), 1994, pp. 329–40.

[14] WANG L.Q., BAER D.R., ENGELHARD M.H., *Creation of variable concentrations of defects on TiO_2(110) using low-density electron beams*, Surface Science **320**(3), 1994, pp. 295–306.

Received November 9, 2004
in revised form January 31, 2005